Available online at www.sciencedirect.com
SCIENCE DIRECT®
Catena 59 (2005) 205–230
CATENA
www.elsevier.com/locate/catena

Surface control of desert pavement pedologic process and landscape function, Cima Volcanic field, Mojave Desert, California

Y.A. Wood[a,*], R.C. Graham[a], S.G. Wells[b]

[a] *Soil and Water Sciences Program, Department of Environmental Sciences, University of California, Riverside, CA 92521-0424, USA*
[b] *Desert Research Institute, Reno, NV 89506, USA*

Received 27 January 2004; received in revised form 1 June 2004; accepted 1 June 2004

Abstract

Desert pavement is a distinctive feature widespread across arid lands of the world. It plays a dynamic role in geomorphic, hydrologic, and ecologic processes. Where desert pavement predominates, infiltration is limited and rainfall is delivered as runoff to nearby bare ground areas where shrubs cluster. Desert pavement surfaces may appear monotonously flat and barren, but we have found, instead, that they are a complex association of landscape and hydrologic elements governed by their surface characteristics. Previously, we identified six unique surface mosaic types that accurately capture the subtle, but distinct, variations in surface clast arrangements for a desert pavement landscape formed on a single-aged basalt flow in the Mojave Desert. We now report that these surface mosaics predict the spatial distribution of fundamental desert vegetation and soil characteristics. Characteristics of soil morphology and texture, the leaching depth of soluble salts, percent plant cover, and shrub species diversity are remarkably consistent for each mosaic type across a 580,000-year-old basalt flow even when measured >1 km apart. Hydrologic character is distinctly different between desert pavement and bare ground regions and vegetation distributions reflect the spatially heterogeneous soil moisture. Where desert shrubs cluster on the three bare ground surface mosaics, leaching is deep, removing most soluble salts to below the 50-cm depth. Where shrubs are absent or few, on the three desert pavement mosaics, leaching depths are shallow, with soluble salt depth

* Corresponding author. Tel.: +1-909-228-0663; fax: +1-909-787-3993.
E-mail address: yvonne.wood@ucr.edu (Y.A. Wood).

0341-8162/$ - see front matter
doi:10.1016/j.catena.2004.06.001

distributions as well as desert shrub percent cover precisely controlled by the percent clast cover of the surface.

Keywords: Desert pavement; Pedogenesis; Leaching; Salinization; Ecology; Aridisols

1. Introduction

In North America, about 50% of natural arid lands is mantled by desert pavement (Evenari et al., 1985), a distinctive surficial feature where at least 65% of the soil surface is clast-covered (Musick, 1975; Wood et al., 2002). The closely packed surface clasts are generally coarse gravel to cobble-sized rock fragments one to two deep that rest on or are embed in underlying soil. Aridisols associated with desert pavement typically have formed in eolian parent material from several centimeters to meters deep immediately underlying the surface clasts (Springer, 1958; Wells et al., 1985, 1995; McFadden et al., 1987). Desert varnish, a hard, dark-colored patina of accumulated iron and manganese oxides, usually covers the surface of the clasts (Krumbein and Jens, 1981; Liu, 2003). From afar, varnished desert pavement makes gently sloping landforms such as alluvial fans, basalt flows, pluvial lake benches, and ancient alluvial terraces (Cooke et al., 1993) appear darkly polished, while up close, it appears as a carefully constructed cobblestone surface.

Wherever found, desert pavement plays a fundamental role in the long-term evolution of the land surfaces it mantles. Surface clasts protect underlying sediments and soil from removal by wind and water (Cooke et al., 1993) and provide a substrate for the capture of eolian sand, silt, clay, and salts. Infiltration is dramatically reduced and precipitation is redirected as runoff to nearby areas free of desert pavement (Abrahams and Parsons, 1991a,b). Additionally, the spatial distribution of desert biota is strongly influenced by desert pavement's primary control of soil water availability (Smith et al., 1995; Dunkerley and Brown, 1995).

The surficial character of desert pavement landscapes is spatially heterogeneous with wide stretches of relatively barren desert pavement (DP) surrounding meter-wide regions of bare ground (BG) where desert shrubs cluster (Musick, 1975). In the eastern Mojave Desert, these two broad landscape types can be further divided into six visually distinct, readily mapped surface mosaics (Fig. 1; Wood et al., 2002). Three surface mosaics (DP1, DP2, and DP3) represent desert pavement regions where surface clast cover is greater than 65%, and three surface mosaics (BG1, BG2, and BG3) represent regions which appear as bare ground with less than 65% surface clast cover (Wood et al., 2002; Fig. 1; Table 1). Across this landscape, these six surface mosaics vary discretely and form heterogeneous patches abutting each other with sharp boundaries of 1- to 10-cm widths. Each mosaic type has a distinctive land surface texture defined by its clast size, degree of clast size sorting, and percent clast cover of the surface (Wood et al., 2002; Fig. 1; Table 1).

Several processes are recognized as playing a role in desert pavement formation (Cooke, 1965; Bull, 1991). However, the capture of eolian sediment between surface

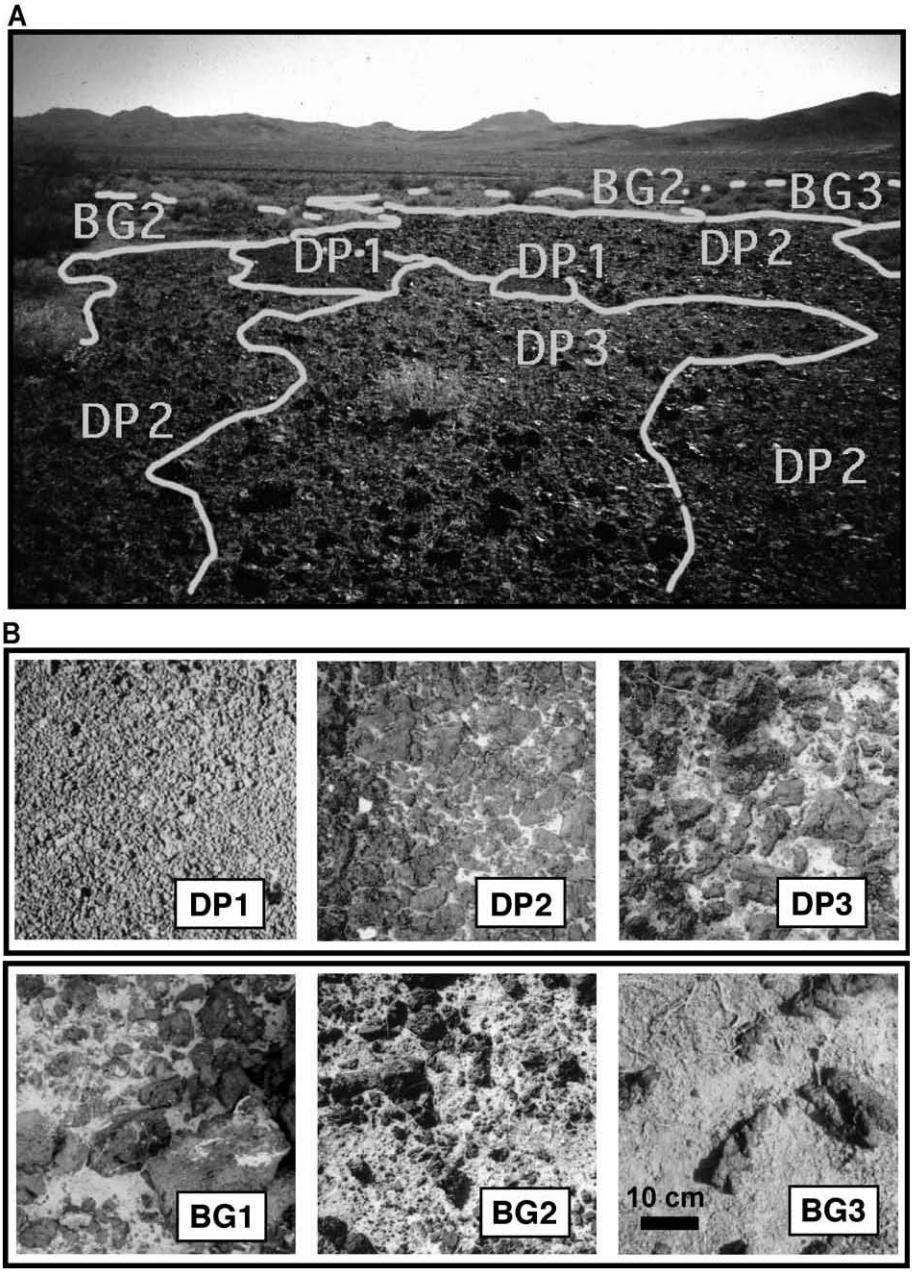

Fig. 1. (A) Surface mosaic types (Wood et al., 2002) delineate the study site's desert pavement landscape into six spatially heterogeneous regions. Surface characteristics of mean clast diameter, percent clast cover of the surface, and degree of sorting co-vary discretely and form a complex array of homogeneous patches that abut each other with sharp boundaries of 1- to 10-cm width. Field of view across front of photograph is approximately 2 m. (B) Plan view photographs of the six surface mosaic types (Wood et al., 2002). Field of view of each photograph is 50 cm. Characteristics of these mosaics are summarized in Table 1.

Table 1
Surface mosaics' physical and vegetative characteristics

Surface mosaic	Clasts			Soil	Shrubs	
	Mean diameter (mm)	Size sorting index	Clast cover (%)	A horizon texture[a]	Shrub cover (%)	Shrub species
Desert pavement						
DP1	12 (1)	0.8 (0.0)	95 (0)	l	0	No shrubs observed.
DP2	22 (2)	1.3 (0.2)	87 (4)	sicl	1.1	*Ambrosia dumosa* *Atriplex hymenelatra** *Larrea tridentata* *Opuntia basilaris*
DP3	45 (6)	1.3 (0.2)	69 (4)	vfsl	5.3	*Atriplex hymenelatra** *Ephedra funerea* *Larrea tridentata* *Lycium andersonnii* *Opuntia basilaris* *Opuntia ramosissima*
Bare ground						
BG1	36 (10)	1.4 (0.2)	54 (12)	ls	8.5	*Ambrosia dumosa* *Atriplex hymenelatra* *Echinocereus triglochidiatus* *Ferocactus cylindraceus* *Larrea tridentata** *Lycium andersonnii* *Mammillaria tetrancistra* *Opuntia basilaris* *Opuntia ramosissima* *Yucca schidigera*
BG2	27 (6)	1.2 (0.3)	58 (9)	scl	27.6	*Ambrosia dumosa** *Atriplex hymenelatra* *Ephedra funerea* *Krameria erecta* *Larrea tridentata** *Lycium andersonnii** *Opuntia basilaris* *Opuntia bigelovii* *Opuntia echinocarpa* *Stephanomeria pauciflora* *Yucca schidigera*
BG3	40 (7)	1.3 (0.2)	21 (7)	fsl	32.3	*Ambrosia dumosa** *Atriplex hymenelatra* *Echinocereus triglochidiatus* *Ephedra funerea* *Ferocactus cylindraceus* *Hymeoclea salsola* *Krameria erecta* *Larrea tridentata* *Lycium andersonnii* *Opuntia basilaris* *Opuntia bigelovii* *Opuntia echinocarpa*

Table 1 (*continued*)

Surface mosaic	Clasts			Soil	Shrubs	
	Mean diameter (mm)	Size sorting index	Clast cover (%)	A horizon texture[a]	Shrub cover (%)	Shrub species
						Opuntia parryi *Opuntia ramosissima* *Yucca schidigera*

Values in parentheses represent standard error. Asterisk indicates dominant/co-dominant shrub species on surface mosaic.

[a] fsl = fine sandy loam; l = loam; ls = loamy sand; scl = sandy clay loam; sicl = silty clay loam; vfsl = very fine sandy loam.

clasts and its translocation into underlying soil has gained widespread acceptance as a major genetic process (Wells et al., 1985, 1995; McFadden et al., 1987; Anderson et al., 2002). We hypothesized that the six surface mosaic types (DP1, DP2, DP3, BG1, BG2, and BG3), each with its own distinctive land surface character, would differentially control pedogenic processes, and thus soil characteristics, across desert pavement landscapes.

2. Material and methods

2.1. Environmental setting

Research was conducted on a desert pavement landscape mantling a 580-ka basalt flow (Turrin et al., 1985) in the Cima Volcanic Field of the eastern Mojave Desert, California. The Pliocene to Holocene Cima volcanic field, comprised of ~ 40 cinder cones and more than 60 associated basalt flows, is host to extensive pedologic, geomorphic, and geochronologic work (Dohrenwend et al., 1984, 1987; Turrin et al., 1985; Farr, 1992; Arvidson et al., 1993; Liu, 2003; Phillips, 2003), including development of the eolian deposition model of desert pavement formation (Wells et al., 1985, 1995; McFadden et al., 1987; Anderson et al., 2002).

The study site is at an elevation of 690 m, approximately 22 km south of Baker, California and 150 km southwest of Las Vegas, NV (Fig. 2). The selected basalt flow, mapped as the e1 flow (Dohrenwend et al., 1984), was chosen because it allows the study of surficial processes on a desert pavement whose lithology (basalt) and time of development (580,000 ± 160,000 years; Turrin et al., 1987) are constant. The physical character of exposed basalt bedrock highs across the site indicates an initial lava flow of blocky morphology. Over time, eolian sediments incorporated into cumulic desert pavement soils (Wells et al., 1985, 1995; McFadden et al., 1987, 1998) have smoothed the original landform's highly variable topographic relief.

The climate is hot and arid as determined by data (National Climatic Data Center, 2003) from six nearby weather stations (Baker, Dunn's Siding, Iron Mountain, Mitchell Caverns, Mountain Pass, and Yucca Grove). The mean annual temperature is calculated to be 20 °C, with a mean annual maximum temperature of 27 °C, and a mean annual minimum

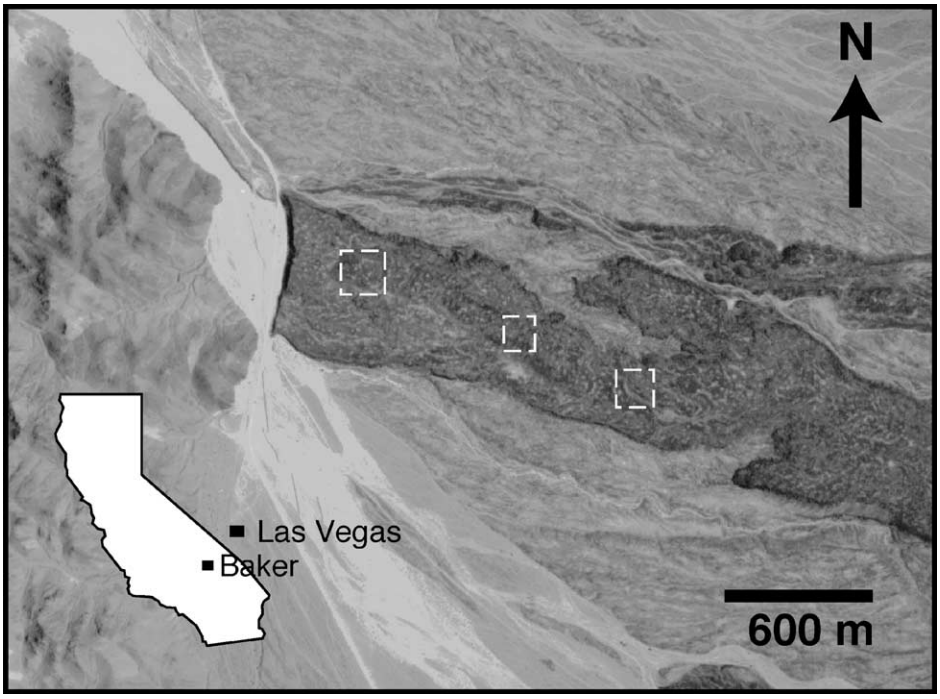

Fig. 2. Vertical aerial photograph shows location of sampling plots on the surface of the 580-ka basalt flow of the Cima volcanic field, eastern Mojave Desert, (35°12′ N; 115°52′ W), approximately 22 km south of Baker, CA. Dark area is basalt flow with surrounding light alluvial fan and wash deposits. Road is vertically trending, white line in the left half of the photograph.

temperature of 13.5 °C. The mean annual precipitation is calculated to be 14 cm, with a bimodal distribution during the year. Most precipitation falls as rain, primarily in the winter months of November through March, with occasional snows. A second smaller peak of precipitation occurs as monsoonal events during the period July through September (National Climatic Data Center, 2003).

Plant cover is generally perennial creosote (*Larrea tridentata*) scrub associations (Billings, 1949; Vasek and Barbour, 1988) with primarily winter annuals (Ludwig et al., 1988).

2.2. Field sampling

Three hectare-size plots previously studied to define desert pavement surface mosaics (Wood et al., 2002) were used in this research. These plots are separated from each other by at least 750 m and were chosen to have no evidence of foot or vehicular travel. Plots were delineated using surface mosaic types (Wood et al., 2002; Fig. 1) and soils were described and sampled within each mosaic type.

Data from previous studies at this site (McFadden et al., 1987; Anderson et al., 2002) showed that an appropriate soil depth to provide evidence of major pedogenic processes

beneath desert pavement was 50 cm. So, within each of the three plots, three 50-cm deep soil pits were described and sampled by morphologic horizon (Soil Survey Division Staff, 1993) in each of five of the six surface mosaics. The sixth mosaic, DP1, covers a minimal area of the landscape and was sampled at only one location. Thus, data were collected from a total of forty-six 50-cm deep soil pits. Based on this sampling protocol, we compared soil physical and chemical features between and within surface mosaic types using data from nine pits for each type distributed across a 2-km region of the basalt flow (Fig. 2).

Desert shrub species identification and percent cover measurements were made using triplicate (one per sampling plot) linear transects which totaled 100-m for each of the six surface mosaics. Measurements of the surface's percent cover by desert forbs and biotic crusts were made using triplicate detailed 1-m linear transects for each sampling plot (a total of nine linear meters per surface mosaic).

2.3. Laboratory analyses

Bulk soil samples were air dried and sieved to remove coarse fragments (>2 mm). Electrical conductivity (EC) values, as an indication of soluble salt content, and pH measurements (Rhoades, 1982) were made of extracts from 1:1 soil/water suspensions from all pits. Particle-size distribution (Gee and Bauder, 1982) was determined by pipette for soil samples from one representative pedon per surface mosaic across the basalt flow. Calcium carbonate equivalent (CCE) (Nelson, 1982) percentages by weight were determined for all soil horizons of three pedons (one per sampling plot) per surface mosaic. Colors of crushed, dry samples for all soil horizons were measured in the laboratory using a chromameter (Minolta Chromameter, Model No. CR-200).

3. Results

3.1. Landscape unit descriptions

The distinctive landscape character of each of the six surface mosaic types is summarized in Table 2 with photographs in Fig. 1. This table combines data previously reported (Wood et al., 2002) with additional data collected in this study.

3.1.1. Desert pavement (DP) surface mosaics

Surface mosaics DP1, DP2, and DP3 define relatively barren (0 to 5% shrub cover) areas for which closely packed clasts (>65% clast cover) predominate as desert pavement. The surface character of each desert pavement mosaic is unique with sharp boundaries of $\leq$10 cm between adjoining mosaic types (Wood et al., 2002).

Surface mosaic DP1 is limited in distribution throughout the study area. Generally, it occurs as 1- to 3-m diameter ovals of moderately sorted clasts inset with sharp boundaries into other DP surface mosaics. Predominately 12-mm-wide subangular gravel almost completely covers (95%) the barren soil (0% shrub cover), making DP1 easy to visually identify in the field.

Table 2
Soil morphological[a] and chemical characteristics of the surface mosaics

Horizon	Depth (cm)	Rock[b] fragments (>2 mm)	Soil[c] texture (<2 mm)	Color[d] (dry, crushed)	Structure[e]	Roots[f]	Pores[f,g]	PH	CCE	Sand	Silt	Clay	Notes
									%Weight				
Mosaic DP1: fine-loamy, mixed, thermic Typic Natrargid													
P[h]	1–0	grmx	–	–	–	–	–	–	–	–	–	–	Angular medium gravel forming desert pavement lies free on surface, with a mean clast size of 12 mm and soil coverage of 95%.
Avk	0–1.5	–	l	1.2Y 6/3	3co col/1fsbk	1f	3m dis v	9.1	NA[i]	NA[i]	NA[i]	NA[i]	Avk and Btk horizons are united together to form distinctive coarse columns (~ 6.5-cm diameter) which can be removed from pit as single units.
Btk	1.5–8	–	c	10YR 6/3	3co col/ 2mabk/ 2vfabk	1vf	–	9.4	NA[i]	NA[i]	NA[i]	NA[i]	
Btkz	8–20	grm	scl	9.8YR 6/3	1msbk	–	–	7.6	NA[i]	NA[i]	NA[i]	NA[i]	
Bkz	20–37	–	sl	9.6YR 6/3	1fsbk/gr	–	–	7.4	NA[i]	NA[i]	NA[i]	NA[i]	
B'tkz	37–50	–	scl	9.4YR 5/3	1fvsbk/gr	–	–	7.1	NA[i]	NA[i]	NA[i]	NA[i]	
Mosaic DP2: fine-loamy, mixed, thermic Typic Natrargid													
P[h]	3–0	grx	–	–	–	–	–	–	–	–	–	–	Angular coarse gravel forming desert pavement lies mostly free; occasionally, it is weakly embedded in top 1 cm of soil. Mean clast size is 22 mm, covering 87% of the soil.

Avk	0–3	–	cl	10YR 6/3	3vc col/1tk pl/2msbk	1vf	3m dis v	9.3 (0.1)	3.9 (2.2)	35	39	27	Avk and Btk horizons are united together to form coarse columns (~ 12-cm diameter) which can be removed from pit as single units with a soil knife.
Btk	2–9	–	cl	9.4YR 6/3	3vc col/3m/ 1f abk	1vf	1f dis t/2vf dis v	8.9 (0.1)	3.4 (1.7)	34	38	29	Fine (<2 mm) crystals of gypsum distributed throughout soil matrix.
Btkz	9–21	grmv	l	9.7 YR 6/3	2fabk/ 1vfsbk	3vf	3vf v	7.7 (0.2)	4.2 (0.7)	39	42	19	
Btkyz	21–30	cb	l	9.4 YR 5/3	1fsbk	1vf	–	7.5 (0.1)	2.1 (0.7)	44	34	21	Soft white masses up to 30 mm in diameter with intact 1–3 mm gypsum crystals.
Btyz	30–37	cbv	sl	9.3 YR 5/3	1fsbk	1vf	–	7.4 (0.1)	1.4 (0.3)	60	21	19	Common soft, white, noneffervescent mottles (gypsum) of ~ 5-mm diameter.
B'tkz	37–50	grc	scl	9.3 YR 5/3	1fsbk	–	–	7.3 (0.1)	1.6 (0.2)	62	15	23	
Mosaic DP3: fine-loamy, mixed, thermic Typic Paleargid													
P^h	3–0	cbx	–	–	–	–	–	–	–	–	–	–	
Av	0–0.5	–	vfsl	1.3 Y 6/3	1mpl	2vf	3f dis ran v	8.4 (0.1)	0.3 (0.3)	68	27	5	Discontinuous Av horizon nestles between pavement clasts. Pores are associated with biotic crusts.
Clasts	0.5–5.5	cbx	–		–			–	–	–	–	–	
Btk	5.5–9.5	–	l	10 YR 6/3	3c/f abk	2vf	3f dis ran v	8.6 (0.2)	0.7 (0.4)	38	38	24	

(continue on next page)

Table 2 (*continued*)

Horizon	Depth (cm)	Rock[b] fragments (>2 mm)	Soil[c] texture (<2 mm)	Color[d] (dry, crushed)	Structure[e]	Roots[f]	Pores[f,g]	PH	CCE	Sand	Silt	Clay	Notes
									%Weight				
Btky	9.5–18	cb	l	9.4 YR 5/3	3c/vf abk	1vf	–	8.8 (0.1)	2.4 (0.5)	50	29	21	Common small (~ 1 mm) crystals (gypsum).
Btkz	18–31	–	cl	9.0 YR 5/3	3fabk/ 2vfsbk	1vf	1vf dis ran v	7.9 (0.3)	2.1 (0.6)	41	31	28	
Btkyz	31–50	–	l	9.1 YR 5/3	3f/vf abk		–	7.9 (0.1)	1.5 (0.6)	43	35	22	Few intact insect casts (~ 10 by 20 mm) with 2-mm-long gypsum needles precipitated inside.
Mosaic BG1: loamy-skeletal, mixed, thermic Typic Calciargid													
Av	0–3	grcv	ls	0.6Y 5/3	1fpl	3vf	2vf v	7.8 (0.1)	1.0 (0.4)	76	20	3	Platy structure influenced by biotic crusts. Deeply embedded angular coarse gravel and cobbles make up 58% of the surface with a mean clast size of 36 mm.
Btk1	3-12	grcv	l	0.3Y 6/3	1f/vf sbk	1vf	3f v	8.2 (0.2)	2.6 (0.9)	50	35	15	Extremely cobbly throughout pit; clast fragments 75% coated by carbonate.
Btk2	12–22	stx	l	10YR 6/3	2f sbk	1vf/1m	3vf v	8.5 (0.2)	5.2 (1.6)	44	35	21	Clast fragments 100% coated by carbonate.
Btk3	22–50	grx	l	10 YR 6/3	1vf sbk	3vf	–	8.7 (0.2)	7.8 (2.3)	50	42	8	Clast fragments 100% coated by carbonate.

Mosaic BG2: fine-loamy, mixed, thermic Typic Haplargid													
Ak	0–2	–	l	1Y 6/3	1co/m pl	3vf	–	7.9 (0.1)	3.8 (2.0)	47	41	12	Horizon depth is influenced by occasional embedded rounded cobbles. Angular, carbonate-encrusted medium gravel provides most of the 58% clast cover, which has a mean clast size of 22 mm.
Bk1	2–5	–	sl	10YR 6/3	2m pr/2f sbk	3vf	3fv	8.0 (0.1)	3.1 (1.8)	53	34	14	
Bk2	5–18	–	sl	10YR 5/3	1f/vf sbk	3vf	2fv	7.9 (0.2)	1.8 (0.9)	56	27	16	
Btk1	18-32	cbv	scl	9.6 YR 5/3	3m sbk/3f abk	2vf	2fv	8.0 (0.2)	1.8 (1.2)	57	22	22	
Btk2	32-50	–	scl	8.7 YR 5/3	3m sbk/3f abk	2vf/2m	3vf ran v	7.9 (0.1)	1.9 (1.2)	58	21	21	
Mosaic BG3: fine-loamy, mixed, thermic Typic Paleargid													
A	0–1	–	sl	0.8Y 6/3	2tkpl/ 2fsbk	2vf	3vf dis ran v & t	7.9 (0.1)	0.3 (0.1)	68	26	5	Rounded surface cobbles are deeply embedded. Mean surface clast size is 40 mm, covering 21% of the soil.
Bw	1–10	–	sl	0.3Y 6/3	1co-msbk	2vf	3f dis ver v and t	7.8 (0.1)	0.1 (0.1)	74	22	4	Occurrence of effervescence spotty.

(continue on next page)

Table 2 (*continued*)

Horizon	Depth (cm)	Rock[b] fragments (>2 mm)	Soil[c] texture (<2 mm)	Color[d] (dry, crushed)	Structure[e]	Roots[f]	Pores[f,g]	PH	CCE	Sand	Silt	Clay	Notes
									%Weight				
Bt1	10–20	cbv	scl	9.1YR 5/3	3csbk/ 1fabk	2vf	2vf dis ran v	7.9 (0.1)	0.3 (0.3)	54	21	25	
Bt2	20–29	cb	scl	8.6 YR 5/3	3f-vf abk/gr	2vf	2vf dis ran v	8.0 (0.3)	0.3 (0.3)	51	21	28	
Btk	29–50	–	scl	8.5YR 5/3	1f-vfabk	1vf	2vf dis ran v	8.2 (0.2)	0.2 (0.2)	47	22	31	Occasional thin threads of carbonate dispersed throughout the matrix.

[a] Soils sampled and described according to Schoeneberger et al., 2002.

[b] c, coarse; cb, cobbly; gr, gravelly; m, medium; st, stony; v, very; x, extremely.

[c] c, clay; cl, clay loam; l, loam; ls, loamy sand; scl, sandy clay loam; sl, sandy loam; vfsl, very fine sandy loam.

[d] Colors measured in Munsell units using a Minolta Chromameter, Model No. CR 200.

[e] 3, strong; 2, moderate; 1, weak; co, coarse; tk, thick; m, medium; f, fine; vf, very fine; abk, angular blocky; col, columnar; gr, granular; pl, platy; sbk, subangular blocky.

[f] 1, few; 2, common; 3, many; f, fine; vf, very fine; m, medium.

[g] v, vesicular; t, tubular; dis, distributed; ran, random; ver, vertical.

[h] P, desert pavement.

[i] NA, value not measured.

Surface mosaic DP2 is extensive in its distribution, comprising about half of all the desert pavement of the study site. The surface clast cover of DP2 (87%) is intermediate between that of DP1 and DP3. The closely packed, generally medium gravel (mean width of 22 mm) is subangular in shape. The gravel clasts may be loosely embedded into the soil, but generally they lie free on the soil surface (Wood et al., 2002). Occasional angular to subangular coarse gravel-size surface clasts are moderately embedded into the soil and may dislodge when walked upon. DP2 supports few shrubs (1% shrub cover), which are predominantly desert holly (*Atriplex hymenelytra*), a halophyte generally found on soil with high salt concentrations (Hunt, 1966).

Surface mosaic DP3 is extensive in its distribution, also comprising about half of all the desert pavement of the study site. DP3 has the least surface cover by clasts (69%) of the desert pavement types and the most surface cover by desert shrubs (5%), with the halophyte desert holly (*A. hymenelytra*) predominating. DP3 is visually distinct from DP2 due to its larger clast size (mean width of 45 mm) and more rounded (subangular to subrounded) clast shape. Surface clasts are firmly embedded in the soil and rarely dislodged when walked upon. In strong contrast to mosaics DP1 and DP2, biotic crusts were observed growing on DP3 soil surfaces.

3.1.2. Bare ground (BG) surface mosaics

Mosaics BG1, BG2, and BG3 delineate surfaces that visually contrast with desert pavement surface mosaics (Figs. 1 and 3). BG surfaces appear to have abundant bare soil, even though more than 50% of the soil surface may be covered by poorly sorted clasts (Table 1; Wood et al., 2002). Generally, the BG mosaics have a more abundant desert shrub cover ($\geq 9\%$), more animal activity, and more biotic crusts than the open DP mosaics.

Surface mosaic BG1 is generally limited to slopes below scattered bedrock highs and has shrub cover (9%) of predominately creosote. In the field, BG1 appears intermediate in physical character between desert pavement and the other two bare ground surface mosaics, and has the greatest range of clast sizes (Table 1). Basalt clasts cover more than half the surface (54%) but are not closely packed to form desert pavement and appear to be rubble from nearby bedrock highs. Many of BG1's angular cobble-size clasts are weakly embedded and often show evidence of recent surficial movement (Wood et al., 2002).

Surface mosaic BG2 generally occurs as 3- to 10-m diameter polygons inset into nearly level regions of desert pavement, often in close association with BG1. This mosaic has a greater concentration of shrubs (28% cover) growing on its nearly level surface than does BG1 on its sloping surface (Fig. 1). Occasional subrounded cobble-size clasts are tightly embedded into the soil. However, most of the surface clasts (58% cover) represent a unique cover, formed by angular to subangular carbonate-encrusted medium and coarse gravel lying free on the surface. This distinctive surface cover distinguishes BG2 from the other two BG mosaics and appears to result from excavations by burrowing mammals (Eghbal and Southard, 1993), which are generally observed only on mosaic BG2.

Surface mosaic BG3 generally occurs as 3- to 10-m diameter polygons inset into other surface mosaics. With the least clast cover (21%), the highest concentration of desert

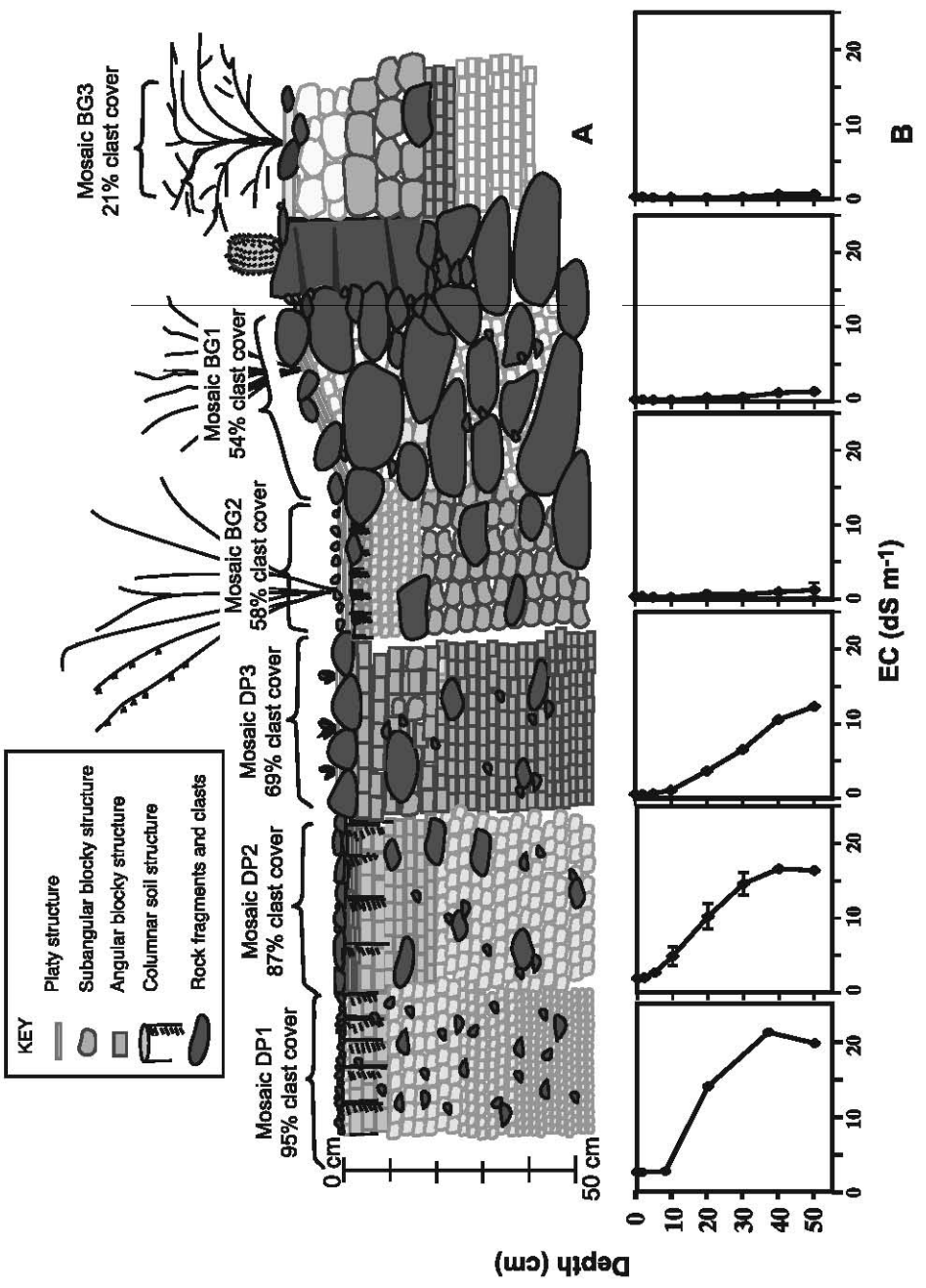
KEY
Platy structure
Subangular blocky structure
Angular blocky structure
Columnar soil structure
Rock fragments and clasts
Mosaic DP1
95% clast cover
Mosaic DP2
87% clast cover
Mosaic DP3
69% clast cover
Mosaic BG2
58% clast cover
Mosaic BG1
54% clast cover
Mosaic BG3
21% clast cover
0 cm
50 cm
A
B
Depth (cm)
EC (dS m-1)

shrubs (32% cover), and the greatest diversity of shrub species growing on its nearly level surface (Table 1), BG3 is easily identified when observed in the field. Subrounded clasts with a mean width of 40 mm are tightly embedded into a soil surface that is mostly free of active mammal burrows. The only evidence of active burrowers is the presence of termite-cast encrusted surface litter in wet years.

3.2. Desert pavement (DP) surface mosaic soils

The soils of the DP surface mosaics have ochric epipedons and very distinctive structure in their top 8 to 10 cm (Fig. 3, Table 2). DP1 and DP2 ('well-developed' pavement with $\geq 80\%$ clast cover) have natric horizons with strong coarse (5- to 10-cm diameter) or very coarse (10- to 16-cm diameter) columns beneath pavement clasts. In contrast, the top 9 cm of DP3, with less clast cover of the surface (69%), has a discontinuous, thin (0.5 to 2 cm deep) surface horizon with weak platy structure nestled between clasts. Immediately below the desert pavement clasts, soil color reddens and clay content increases, forming a distinctive morphologic feature of mosaic DP3. For all three DP mosaics, morphologic evidence of gypsum, high EC values (Fig. 3, Table 2), and argillic (or clay-enriched) soil horizons are distinctive subsurface features.

3.2.1. Surface mosaic DP1 soil (fine-loamy, mixed, thermic Typic Natrargid)

Strong, coarse columns immediately underlie the pavement. They can be removed intact and easily separated along a clear structural and color boundary into an uppermost thin (1.5 cm) loamy Avk horizon and an underlying clayey Btk horizon ($\sim$ 6 cm thick). Beneath these columns, several soil characteristics dramatically change. The EC increases up to six-fold (Fig. 3) with the soil becoming saline by the 10-cm depth. Roots are no longer observed, soil texture becomes sandier, soil color reddens, and soil structure weakens (Table 2).

3.2.2. Surface mosaic DP2 soil (fine-loamy, mixed, thermic, Typic Natrargid)

The near surface soil morphology of DP2 is similar to that of mosaic DP1. Closely packed surface clasts rest on strong soil columns, comprising the Avk and Btky horizons. The columns are at least twice as wide as those of DP1 (10 to 16 cm in diameter) and just as deep (8 to 10 cm deep). The Avk horizon is 3 cm thick, has clay loam texture, and weak thick (1 cm) structural plates that break to moderate, medium subangular blocky structure. The Btk horizon, forming the lower part of the columns, is redder, has strong, medium angular blocky structure, and fine (<2 mm) crystals of gypsum distributed throughout the matrix.

Fig. 3. (A) Schematic diagram shows the relations between mosaics and soil morphology. Sites selected by surface mosaic type produce predictable soil structure characteristics unique to that mosaic, even though sampling sites may be separated by >1 km. The subsurface boundaries between surface mosaic soil types are gradual, rather than abrupt as represented here. (B) Electrical conductivity values of soil extracts plotted to the 50-cm depth to indicate soluble salt concentration (Rhoades, 1982) under each of the surface mosaic soil types. Bars indicate standard error values; $n=9$ at each depth except for mosaic DP1 ($n=1$).

As with DP1, several soil characteristics change dramatically just beneath the columns. Soluble salts increase, with the soil becoming saline at the 10-cm depth and EC values doubling from 5 to 10 dS m^{-1} by the 20-cm depth (Fig. 3). Very fine roots become more numerous, soil texture becomes sandier, and soil structure weakens.

3.2.3. Surface mosaic DP3 soil (fine-loamy, mixed, thermic Typic Paleargid)

The surface soil morphology of DP3 contrasts with that of DP1 and DP2 in that no soil columns are present. Instead, a thin (0.5 to 2 cm deep), discontinuous Av horizon of sandy loam texture is nestled between surface clasts tightly embedded 2 to 3 cm deep into an underlying Btk horizon. Both the weak platy Av and strong blocky Btk are well leached (EC < 1 dS m^{-1}) to the 10-cm depth (Fig. 3). The soil becomes saline at the 20-cm depth as EC values increase to a mean of 12.5 dS m^{-1} at the 30–50-cm depth. Concurrently, soil color reddens and angular blocky soil structure remains strong. Below 30 cm, roots are no longer observed.

3.3. Bare Ground (BG) surface mosaic soils

In contrast to the DP mosaics, BG surface mosaics generally have little measurable soluble salt and no morphological evidence of the presence of gypsum throughout their 50-cm depths. However, here are seen the least and most accumulations of soil carbonate within the surface 50-cm depth as measured by CCE (Table 2) across the landscape. Below sandy ochric epipedons with weak platy soil structure, soil texture increases in clay content and structure increases in strength at some point with depth to 50 cm.

3.3.1. Surface mosaic BG1 soil (loamy-skeletal, mixed, thermic Typic Calciargid)

A predominance of calcium carbonate-covered ($\geq$ 75% coated) rock fragments forms a distinctive feature of BG1 soils throughout the 50-cm depth. These clasts are mainly cobbles, with material < 2 mm providing only 10% to 15% of the soil volume. Carbonate accumulates within the nonsaline soil and CCE increases from 2% to 10% (Table 2) by the 40-cm depth.

The thin, sandy Av surface horizon has weak platy structure associated with the many very-fine roots and hyphae distributed throughout its 3-cm depth. Below the Av horizon, roots decrease in number as clay content increases and soil color reddens. Soil structure strengthens from the 10- to 20-cm depth where clay content is the greatest, but weakens again below the 20-cm depth as soil clay content decreases and fine roots increase in number.

3.3.2. Surface mosaic BG2 soil (fine-loamy, mixed, thermic Typic Haplargid)

Weak platy structure of the loamy Ak horizon contrasts with the moderately strong soil prisms ($\sim$ 5-cm diameter) of the underlying reddened Bk horizon. Within the 5-cm depth, CCE values are the highest measured in BG2 soils (3% to 4%, Table 2). Beneath the 5-cm depth, structure is weak subangular blocky until below the 18-cm depth where clay content increases, soil color reddens, soil structure becomes strong subangular blocky, and CCE values decrease to < 2% (Table 2). Here, very fine roots lessen in quantity and are generally confined to between the subangular structural blocks.

3.3.3. Surface mosaic BG3 soil (fine-loamy, mixed, thermic Typic Paleargid)

The loamy soils of BG3 are predominantly free of accumulations of soluble salts or soil carbonates to the 50-cm depth (Fig. 3, Table 2). The thin (1 cm) A horizon has slight effervescence in parts (CCE of 0.3%) and forms moderately strong, thick structural plates. Below the 10-cm depth, soil color reddens, clay is enriched, and angular blocky structure becomes strong. Below the 30-cm depth, limited carbonate (CCE = 0.3%) forms violently effervescent white threads throughout the brown sandy clay loam soil, angular blocky structure becomes weak, and root counts decrease (Table 2).

4. Discussion

4.1. Surface clast control of landscape-scale soil water

The depth of soil water movement and solute transport is strongly tied to surface clast character differences across the landscape (Fig. 3, Table 3). Measured EC values at all soil depths except 5–10 cm correlate at a statistically significant level ($p < 0.05$) to percent clast cover (Table 3). That is, soluble salts, carried by the wind from nearby playas (Reheis et al., 1989; Reheis and Kihl, 1995) and deposited on the surface in desert dust, are concentrated at shallower depths as percent clast cover increases (Table 3, Fig. 3). The three DP surface mosaics (clast cover >65%) have shallow leaching regimes with soluble salts accumulated near the land surface (Fig. 3). In contrast, the three BG surface mosaics (clast cover < 65%) have deep leaching regimes that prevent the accumulation of soluble salts within the surface 50-cm depth.

4.1.1. Desert pavement subsurface hydrologic regimes

Deeper leaching regimes of the three BG surface mosaics (Fig. 3) suggest regions where infiltration of rainwater is unimpeded—or regions of focussed recharge. In contrast, surface run-off predominates on the DP surface mosaics (Musick, 1975; Wilcox et al., 1988; Abrahams and Parsons, 1991a,b) and soluble salts have accumulated at shallow

Table 3
Regression values indicating correlations between surface mosaic characteristics and soil solution EC with soil depth ($n = 6$)

Soil depth (cm)	ANOVA correlation to saturated paste EC					
	Clast cover (%)		Clast width (mm)		Sorting index	
	r^2	p	r^2	p	r^2	p
0–2	**0.99**	0.0004	**0.86**0.034	0.56	0.29	
2–5	**0.95**	0.012	0.72	0.147	0.38	0.49
5–10	0.84	0.066	0.53	0.32	0.19	0.73
10–20	**0.99**	< 0.0001	0.84	0.062	0.56	0.29
20–30	**0.99**	0.0005	0.85	0.060	0.58	0.28
30–40	**0.95**	0.013	0.71	0.154	0.41	0.45
40–50	**0.91**	0.027	0.69	0.176	0.38	0.49

Statistically significant correlations are shown in bold.

depths (Fig. 3). The depth of leaching is precisely governed by clast cover character (Table 3) and each of the three DP mosaics represents a separate region of distinct hydrologic character (Fig. 3) even though separated by boundaries of only a few centimeters (Fig. 1). For instance, the depth at which sufficient soluble salts have accumulated to produce EC values greater than 12 dS m^{-1} varies distinctly between the three DP mosaics. For DP1, this depth is 8 cm as very limited rainwater infiltrates. For DP2, this depth is 20 cm. And for DP3, this depth is 40 cm as water freely infiltrates into the top 10 cm of the soil.

4.1.2. Shrub distributions across desert pavement landscapes

As percent clast cover of the surface increases, measured biotic characteristics of plant cover ($r^2 = 0.98$) and desert shrub species richness ($r^2 = 0.92$) decrease (Fig. 4A). Since available water is the primary limit on desert plant growth, this relationship reflects the precise control of soil moisture by closely juxtaposed differences in clast cover. For instance, DP1 (95% clast cover) is consistently barren, whereas mosaic DP3 (69% clast cover) has 5% shrub cover. On BG mosaics, the presence of clustered shrubs (shrub cover $\geq 9\%$) reflects higher soil moisture.

While all three BG mosaics are regions of focussed soil moisture recharge where salts are leached below the 50-cm depth, the amount of plant cover is still tightly linked to surface clast cover percentage (Fig. 4A). The phenomenon of percent shrub cover being strongly correlated to percent clast cover has been observed throughout North American deserts when data collected from different aged land surfaces are compared (Fig. 4B). Our observation of this trend on a single-aged landform reflects the universality of control of subsurface hydrology, soil moisture, and vegetation distributions by the clast cover. This suggests that the physical character of the top few centimeters of arid land surfaces is core in determining the spatial distribution of water across arid landscapes, independent of landform, or soil, age.

4.2. Spatially disjunct patterns of soil genesis

4.2.1. Mosaic DP1

For DP1 mosaics, where infiltration rates are low and desert shrub cover is absent, the predominant soil-forming factor is the physical incorporation of salts and other eolian materials within the soil. Eolian sand and desert dust (silt, clay, and salt) are predominantly trapped by surface clasts and transported down between coarse surface columns (McFadden et al., 1987; Anderson et al., 2002), especially when the soil is dry and wide cracks are present (Hugie and Passey, 1964). During large storm events, rainwater is shed from covering clasts and channeled by soil column faces (Coen and Wang, 1989; Lin et al., 1999) to a depth of 8 cm, carrying soluble salts in solution and sand, silt, and clay in suspension (Weisbrod et al., 2000; Anderson et al., 2002). These materials then accumulate near the base of the columns. Here, channeled water movement is slowed as the weak blocky structure of the underlying Btkz horizon offers fewer interpedal conduits for continued flow (Coen and Wang, 1989).

The clayey soil of the Btk horizon (forming the bottom two thirds of the columns) eventually wets and swells, closing the interpedal cracks. The rate of water moving into the soil is greatly reduced (Reid et al., 1993; Lin et al., 1998), confining most added

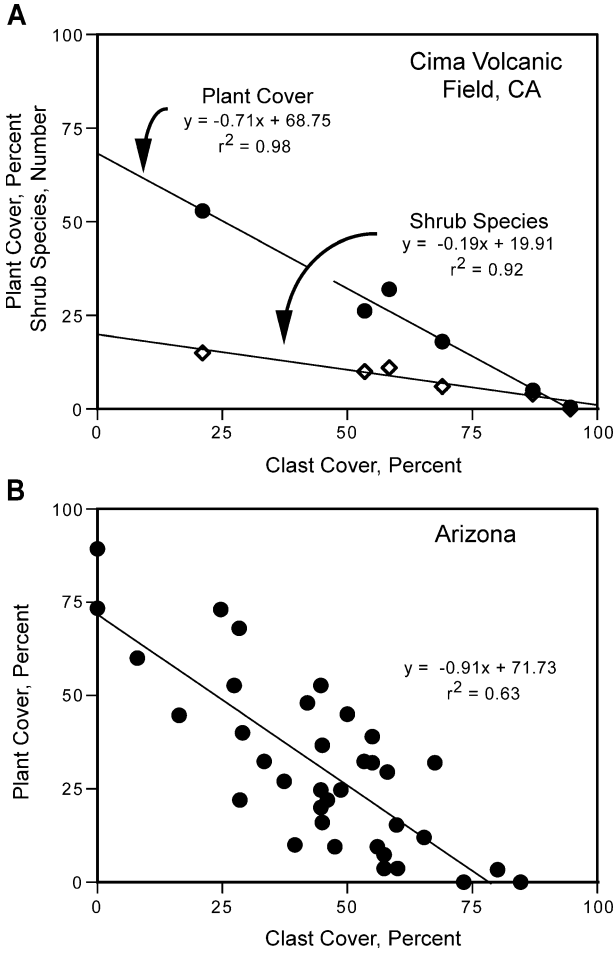

Fig. 4. (A) Desert vegetation characteristics of cover (shrubs and ephemerals) and shrub species diversity highly correlate with percent clast cover across the Cima volcanic field desert pavement landscape. Values on the *y*-axis reflect both number of plant species and percent plant cover of the surface. (B) The phenomenon of plant cover correlating strongly with surface clast cover is well documented in other North American deserts (Tromble et al., 1974; Wilcox et al., 1988; Abrahams and Parsons, 1991b; Parsons et al., 1992). Data compiled in Arizona (Tromble et al., 1974; Abrahams and Parsons, 1991b; Parsons et al., 1992) reflect this trend by comparing results taken from several locales on different-aged landforms.

material to within the columns (Anderson et al., 2002). This allows the accumulation of wind-deposited salts important to arid-land pedogenic process, including very soluble chlorides and sulfates, sodium and magnesium carbonates, gypsum, and calcium carbonate (Reheis et al., 1989; Reheis and Kihl, 1995), within the top 10-cm depth of the soil surface (Fig. 3). The soil is saline (4 dS m^{-1}) by the 10-cm depth, and the few observed fine and very fine roots extend only to the 8-cm depth, restricted from further growth by high salinity.

Very alkaline soil (pH of 9.1) to the 5-cm depth indicates the accumulation of sodium carbonate (Na_2CO_3) within the top 5 cm of the columns (Szabolcs, 1979). This in turn promotes sodium saturation of clay minerals, enhanced soil swelling, poor drainage, and prismatic structure (Munn and Boehm, 1983). While field morphology indicates that some soil carbonates are illuviated beneath surface columns (Table 2), measured pH drops to less than 7.6 below the 5-cm depth, indicating solutions containing predominantly neutral salts such as chlorides or sulfates (Szabolcs, 1979). Some of these salts are very soluble, and their dissolution into the limited water entering DP1 increases the ionic strength of the soil solution. This in turn limits the dissolution of the lesser soluble sodium and calcium carbonates deposited as dust, limiting their illuviation to depth.

4.2.2. Mosaic DP2

Similar to DP1, the Avk and Btk horizons of DP2 unite to form strong columns within the top 9 cm of soil. The Avk horizon of DP2 has CCE values near 4% with strong soil alkalinity (pH = 9.3) indicating the presence of Na_2CO_3 to the 5-cm depth. This suggests limited dissolution and translocation of the $CaCO_3$ deposited as dust on the land surface, since it is much less soluble than Na_2CO_3. Similar to DP1, high clast cover of the surface limits the bare soil available to directly intercept incoming rainwater. Increased water shed from surface clasts onto decreased regions of open soil channels water rapidly down the cracks formed in the dry soil (Hugie and Passey, 1964). Clay loam textures within the columns reflect the slowing of water as cracks swell shut during rain events and clays deposited as desert dust are incorporated in the soils of the columns (Anderson et al., 2002) above the 9-cm depth.

Below the boundary of these very coarse columns sand content and soluble salt concentrations increase. Moderately strong angular blocky structure found below 10 cm continues to provide interpedal pores for water movement to a depth of 20 cm where measured EC jumps to 10 dS m^{-1} (Fig. 3). Here, weak structure slows water movement (Lin et al., 1999), and gypsum and very soluble salts precipitate to form Btkyz horizons. This represents a less steep increase in soluble salts compared to DP1 where EC values increase from 2.5 to 14 dS m^{-1} by the 20-cm depth (Fig. 3). As soil water movement decreases within the 10- to 20-cm depth, translocated calcium carbonate also accumulates as indicated by the pH of 7.7 and CCE values of 1% to 2%. Here, the strong ionic activity of soil solutions enriched in soluble salts acts to limit the dissolution and further transport of carbonates (McBride, 1994).

4.2.3. Mosaic DP3

The sandy loam Av horizon nestled between surface clasts reflects the ability of DP3, unique among the desert pavement types, to capture and retain eolian sand. Thus, the Av horizon of DP3 not only has more surface area (14%) for the direct intercept of rainwater than mosaics DP1 and DP2, but its soil texture is also more sandy—68% sand compared to 35% for DP2 (Table 2). Water infiltrates rapidly into sandy soil (Yair et al., 1997), leaching soluble salts deposited on the surface. The near absence of soluble salts within the top 10 cm of DP3 (soil extracts are $\leq$1.1 dS m^{-1}) reflects such free leaching. Once beneath the surface clasts, infiltrating water readily flows through the

interpedal pores associated with strong angular blocks (Lin et al., 1999) and the subsurface soil does not become saline until below the 20-cm depth, where soil structure is weaker.

The pH values near 8.5 to the 5-cm depth indicate solutions containing dissolved $CaCO_3$. However, CCE values are low, less than 0.5%, with most carbonates deposited as dust being leached deeper, in contrast to DP1 and DP2. From the 20- to 30-cm depth, CCE increases to 2% and pH increases to near 9 suggesting the presence of accumulated Na_2CO_3. Here, EC values increase to near 4 dS m^{-1}, and the higher ionic strengths should favor the precipitation of carbonates carried in solution. From the 30- to 50-cm depth, pH of 7.8 to 8.2 indicates the presence of neutral salts and $CaCO_3$ as the dominant soil carbonate.

4.2.4. Mosaic BG1

Mosaic BG1 is a region of the landscape where calcium carbonate and sand accumulate. The Av horizon of BG1 has the sandiest textures across the landscape (76% sand, Table 2), due to efficient sand trapping by a very rocky substrate inherited from rubbled basalt outcrops. Beneath the sandy loam A horizon, the large number of rock fragments forms an open network of macropores for the movement of soil water, leaching soluble salts to below the 50-cm depth (EC values ≤ 1 dS m^{-1}). The accumulation of $CaCO_3$ is indicated by soil solution pH values ranging from 7.8 to 8.7, rock fragments that are 100% carbonate covered below the 10-cm depth, and CCE values increasing from 2% to >10% with depth.

Many roots extend throughout the 50-cm depth of the pits, increasing macropore channels for water flow (Tyler et al., 1994), and promoting the translocation of clays and carbonate. Clay translocation can be slowed by the presence of $CaCO_3$ in solution (Goss et al., 1973; Doner and Lynn, 1989). The particle size distribution of soil material <2 mm indicates that clay has been translocated for the entire depth of the BG1 pits. However, maximum clay accumulations occur between the depths of 10 and 20 cm, just above where CCE values begin to increase rapidly (Table 2).

4.2.5. Mosaic BG2

Pedogenesis in BG2 is primarily controlled by surface additions of eolian sand accumulating in the wind shadow of desert shrubs, and the redistribution of clay and carbonates from below 20 cm onto the soil surface by burrowing mammals. Clumps of desert shrubs (27% cover) increase surface roughness and trap eolian sand (Barth and Klemmedson, 1978) that is incorporated to the 50-cm depth. Low EC values, pH values of 7.9 to 8.1, and CCE values between 2% and 4% indicate the accumulation of $CaCO_3$ but the absence of soluble salts, including Na_2CO_3, as soil water readily leaches to below the 50-cm depth (Fig. 3, Table 2). Strong effervescence and CCE values of $\sim$ 4% within platy Ak horizons indicate that carbonates are concentrated near the surface (Table 2). Below the top 5 cm of BG2, CCE values are near 2% to the 50-cm depth, suggesting the redistribution of soil carbonate to the surface by burrowing mammals (Eghbal and Southard, 1993). Such bioturbation also explains the higher clay content of BG2 surface soils compared to BG1 and BG3 (Table 2), as well as the presence of the distinctive carbonate-coated medium gravel covering the surface of BG2.

4.2.6. Mosaic BG3

Plants exert their greatest pedogenic effect here where shrub cover is 32%. Clumped desert shrubs increase the surface roughness of BG3 and trap windblown sand, which is incorporated into the Avk and Btk horizons (Lyford and Qashu, 1969; Rostagno, 1989; Rostagno et al., 1991). Neither soluble salts nor carbonates accumulate appreciably within the top 50 cm of BG3 as water readily moves to below this depth (Fig. 3). Overall, sandy loam soil textures and macropore channels from shrub roots promote deep preferential flow and clay illuviation to below the 20-cm depth in mosaic BG3. Additionally, the clustered shrubs influence soil structure through the additions of organic material and acids within the rooting zone.

4.3. Origin and development of surface mosaic heterogeneity across desert pavement landscapes

Processes responsible for the origin and development of the distinctive physical character of each of the six surface mosaics are not fully understood at this time. However, spatial distributions of surface mosaics formed on other basalt flows in the Cima volcanic field suggest that the initial morphology and topography of a landform influence the evolving patterns of surface mosaics across desert pavement landscapes. For instance, surface mosaics studied in this work are compact and rounded when compared to those mantling an adjoining lava flow which are widespread and elongate. This neighboring flow has basalt indicative of an original pahoehoe lava morphology whose topography was elongate and smooth. In contrast, the flow forming the basis of this study has basalt indicative of an original aa morphology whose topography was blocky and rough.

Over time as surface topography becomes increasingly smoothed, the dominant processes forming surface mosaics may vary. For example, the pedogenic accumulation of soluble salts high in the solum and concomitant salt fracturing of surface clasts represents a dominant process in the development of surface mosaic DP2. On the other hand, the predominance of $\sim$ 1 cm diameter gravels on surface mosaic DP1 (Table 1) may result from the slow infilling of previously clast-free regions by waterborne gravels (Haff and Werner, 1996; Wood et al., 2002). Such infilled polygons may record past surficial disturbances, perhaps from the presence of plant cover and associated burrowing animals, as long as 5000 years ago (Wood et al., 2002).

5. Conclusions

5.1. Spatial partitioning of surficial processes by clast cover character

This study identifies the patterning of clast cover as the dominant control of water and sediment distribution across and into this arid landscape. This control operates at a scale of decimeters, precisely determining soil morphology, subsurface hydrologic regimes, and ecosystem components. Seemingly subtle, but distinct, variations in the texture and fabric of surface clast cover translate into profound differences in the underlying soils and associated plant communities of desert pavement landscapes. Throughout the formation of

this desert pavement landscape, and continuing today, surface physical character has closely controlled rainfall redistribution, the movement of water, salts, and clays into the subsurface, and the spatial distribution of vegetative cover. That is, a thin layer of surface clasts and soil, directly intersecting the atmosphere, dynamically and precisely determines surficial processes across this desert land surface yielding a close genetic relationship between the landscape, soilscape and ecosystem.

5.1.1. Control of pedogenic processes

Soluble salts and carbonates accumulate at different depths within the soil of each surface mosaic type (Fig. 3; Table 2), reflecting spatially disjunct patterns of pedogenic process across the landscape. Inputs of precipitation and eolian materials are consistent across the studied land surface, but rates and types of pedogenic processes incorporating them into soil are not. Subsurface soil morphology to the 50-cm depth—a readily observed feature in the field—is distinct for each mosaic (Fig. 3A) reflecting long-term precise spatial partitioning of surficial processes. Over time, each mosaic's soil morphology has evolved and reinforced itself as important pedogenic processes of eolian sediment additions and translocation, and the infiltration and subsurface flow of soil water are controlled by its surface's character. Differences in soil morphology are sufficient that classifications of soils from within abutting mosaic types vary at a high taxonomic level, from Haplargids to Paleargids.

5.1.2. Control of hydrologic and ecologic processes

The studied desert pavement landscape has four regions of distinct hydrologic character. Across the complex array of six surface mosaics, rainwater will be redistributed differentially for each type, yielding in turn a complex array of soil moisture regimes that precisely govern desert plant distributions and associated pedogenic process. Vegetative cover ranges from that of only scarce ephemerals where clast cover and concentrated soil salts are high, to as much as 50% combined coverage by vascular plants where clast cover is low and leaching is to the 50-cm depth.

5.2. Surface character and desert pavement landscape evolution

These findings are important to an understanding of the evolution of desert pavement landscapes. The close relationship of land surface character with water movement, soil development, and biotic distributions is indicative of a system whose components have co-evolved through sensitive feedback systems. Surface clast control of leaching depths plays two important roles in the functioning of this arid landscape. First, salt-enriched DP soils limit rooting depth (Munns and Termaat, 1986) and reduce shrub species diversity to primarily salt tolerant halophytes (Fig. 4; Table 1; Vasek and Barbour, 1988; Hickman, 1993). In contrast, relatively salt-free BG mosaics support the most shrub cover and species diversity across the landscape (Fig. 4).

Second, where high salt contents are observed near the soil surface, increased physical weathering of surface clasts due to salt fracturing (Smith and McGreevy, 1983; Amit et al., 1993) is expected. Near-surface salt concentrations are high in mosaics DP1 and DP2 (Fig. 3), the only location where salt fracturing has been observed in the

field. Through time, surface clast fracturing increases both clast numbers and the amount of clast cover, fostering a feedback mechanism in which increasing clast cover decreases leaching depths and soil moisture. This further concentrates soluble salts close to the surface, thereby decreasing plant cover and removing available root conduits for subsurface water flow.

Acknowledgements

We are grateful to Joan Breiner, Jean Graham, Carrie-Ann Houdeshell, Brad Lee, Lynn Moody, Kathy Rose, Sylvie Quideau, and April Ulery for invaluable field assistance, animated discussions, and companionship. We thank Dr. Martin A.J. Williams and an anonymous reviewer for helpful editorial comments. Additionally, we thank the National Park Service for permission to conduct this study on their land, and the Zzyzx (California State University) and the Granite Mountains (University of California) research stations staff for advice, technical support and welcome shelter. Y.A.W. gratefully acknowledges the financial support of the University of California, Riverside, in the form of graduate student travel grants and fellowship awards. Additionally, she is honored by the recognition of the California Desert Consortium through its award of the Judith Presch Fellowship and of the Desert Research Institute through its award of the Jonathan O. Davis Fellowship.

References

Abrahams, A.D., Parsons, A.J., 1991a. Relation between infiltration and stone cover on a semiarid hillslope, southern Arizona. Journal of Hydrology 122, 49–59.

Abrahams, A.D., Parsons, A.J., 1991b. Relation between sediment yield and gradient on debris-covered hillslopes, Walnut Gulch, Arizona. Geological Society of America Bulletin 103, 1109–1113.

Amit, R., Gerson, R., Yaalon, D.H., 1993. Stages and rate of the gravel shattering process by salts in desert Reg soils. Geoderma 57, 295–324.

Anderson, K.A., Wells, S.G., Graham, R.C., 2002. Pedogenesis of vesicular horizons, Cima volcanic field, Mojave Desert, California. Soil Sci. Soc. Am. J. 66, 878–887.

Arvidson, R.E., Shepard, M.K., Guinness, E.A., Petroy, S.B., Plaut, J.J., Evans, D.L., Farr, T.G., Greeley, R., Lancaster, N., Gaddis, L.R., 1993. Characterization of lava-flow degradation in the Pisgah and Cima volcanic fields, California, using Landsat Thematic Mapper and AIRSAR data. Geological Society of America Bulletin 105, 175–188.

Barth, R.C., Klemmedson, J.O., 1978. Shrub-induced spatial patterns of dry matter, nitrogen and organic carbon. Soil Science Society of America Journal 42, 804–809.

Billings, W.D., 1949. The shad scale vegetation zone of Nevada and eastern California in relation to climate and soils. American Midland Naturalist 42, 87–109.

Bull, W.B., 1991. Geomorphic Responses to Climatic Change. Oxford Univ. Press, Oxford.

Coen, G.M., Wang, C., 1989. Estimating vertical saturated hydraulic conductivity from soil morphology in Alberta. Canadian Journal of Soil Science 69, 1–16.

Cooke, R., 1965. Desert pavement. Mineral Information Service 18, 197–200.

Cooke, R., Warren, A., Goudie, A., 1993. Desert Geomorphology. UCL Press, London.

Dohrenwend, J.C., McFadden, L.D., Turrin, B.D., Wells, S.G., 1984. K–Ar dating of the Cima volcanic field, eastern Mojave Desert, California: Late Cenozoic volcanic history and landscape evolution. Geology 12, 163–167.

Dohrenwend, J.C., Abrahams, A.D., Turrin, B.D., 1987. Drainage development on basaltic lava flows, Cima volcanic field, southeast California, and Lunar Crater volcanic field, south–central Nevada. GSA Bulletin 99, 405–413.

Doner, H.E., Lynn, W.C., 1989. Carbonate, halide, sulfate, and sulfide minerals. In: Dixon, J.B., Weed, S.B. (Eds.), Minerals in Soil Environments. Soil Science Society of America Book Series: Number One, Second Edition. ASA, Madison, WI, pp. 279–330.

Dunkerley, D.L., Brown, K.J., 1995. Runoff and run on areas in a patterned chenopod shrubland, arid western New south Wales, Australia: characteristics and origin. Journal of Arid Environments 30, 41–55.

Eghbal, M.K., Southard, R.J., 1993. Micromorphological evidence of polygenesis of three Aridisols, western Mojave Desert, California. Soil Science Society America Journal 57, 1041–1050.

Evenari, M., Noy-Meir, I., Goodall, D.W., 1985. Hot Deserts and Arid Shrublands: Part A. Elsevier, New York.

Farr, T.G., 1992. Microtopographic evolution of lava flows at Cima volcanic field, Mojave Desert, California. Journal of Geophysical Research 97 (B11), 15171–15179.

Gee, G.W., Bauder, J.W., 1982. Particle-size analysis. In: Page, A.L., Miller, R.H., Keeney, D.R. (Eds.), Methods of Soil Analysis: Part 2. Agronomy Monographs: No. 9, 2nd ed. ASA, Madison, WI, pp. 383–411.

Goss, D.W., Smith, S.J., Stewart, B.A., 1973. Movement of added clay through calcareous materials. Geoderma 9, 97–103.

Haff, P.K., Werner, B.T., 1996. Dynamical processes on desert pavement and the healing of surficial disturbances. Quaternary Research 45, 36–46.

Hickman, J.C., 1993. The Jepson Manual: Higher Plants of California. Univ. of California Press, Berkeley, CA.

Hugie, V.K, Passey, H.B., 1964. Soil surface patterns of some semiarid soils in northern Utah, southern Idaho, and northeastern Nevada. Soil Science Society Proceedings 28, 786–792.

Hunt, C.B., 1966. Plant ecology of Death Valley, California. U.S. Geological Survey Professional, 509.

Krumbein, W.E., Jens, K., 1981. Biogenic rock varnishes of the Negev Desert (Israel), an ecological study of iron and manganese transformation by cyanobacteria and fungi. Oecologia (Berlin) 50, 25–38.

Lin, H.S., McInnes, K.J., Wilding, L.P., Hallmark, C.T., 1998. Macroporosity and initial moisture effects on infiltration rates in vertisols and vertic intergrades. Soil Science 163, 2–8.

Lin, H.S., McInnes, K.J., Wilding, L.P., Hallmark, C.T., 1999. Effects of soil morphology on hydraulic properties: I. Quantification of soil morphology. Soil Science Society of America Journal 63, 948–954.

Liu, T., 2003. Blind testing of rock varnish microstratigraphy as a chronometric indicator: results on late Quaternary lava flows in the Mojave Desert, California. Geomorphology 53, 209–234.

Ludwig, J.A., Cunningham, G.L., Whitson, F.D., 1988. Distribution of annual plants in North American deserts. Journal of Arid Environments 15, 221–227.

Lyford, F.P., Qashu, H.K., 1969. Infiltration rates as affected by desert vegetation. Water Resources Research 5, 1373–1376.

McBride, M., 1994. Environmental Chemistry of Soils. Oxford Univ. Press, Oxford.

McFadden, L.D., Wells, S.G., Jercinovich, M.J., 1987. Influences of eolian and pedogenic processes on the origin and evolution of desert pavements. Geology 15, 504–508.

McFadden, L.D., McDonald, E.V., Wells, S.G., Anderson, K.C., Quade, J., Forman, S.L., 1998. The vesicular layer and carbonate collar of desert soils and pavements: formation, age and relation to climate change. Geomorphology 24, 101–145.

Munn, L.C., Boehm, M.M., 1983. Soil genesis in a Natrarid-Haplargid complex in northern Montana. Soil Science Society of America Journal 47, 1186–1192.

Munns, R., Termaat, A., 1986. Whole plant response to salinity. Australian Journal of Plant Physiology 13, 143–160.

Musick, H.B., 1975. Barrenness of desert pavement in Yuma County, Arizona. Arizona-Nevada Academy of Sciences Journal 10, 24–28.

National Climatic Data Center, 2003. NCDC Website, National Oceanic and Atmospheric Administration, United States Department of Commerce (http://www.ncdc.noaa.gov).

Nelson, D.W., 1982. Carbonate and gypsum. In: Page, A.L., Miller, R.H., Keeney, D.R. (Eds.), Methods of Soil Analysis: Part 2. Agronomy Monographs: No. 9, 2nd ed. ASA, Madison, WI, pp. 181–197.

Parsons, A.J., Abrahams, A.D., Simanton, J.R., 1992. Microtopography and soil-surface materials on semi-arid piedmont hillslopes, southern Arizona. Journal of Arid Environments 22, 107–115.

Phillips, F.M., 2003. Cosmogenic ^{36}Cl ages of Quaternary basalt flows in the Mojave Desert, California, USA. Geomorphology 53, 199–208.

Reheis, M.C., Kihl, R., 1995. Dust deposition in southern Nevada and Californian, 1984–1989: relations to climate, source area, and source lithology. Journal of Geophysical Research 100 (5), 8893–8918.

Reheis, M.C., Harden, J.W., McFadden, L.D., Shroba, R.R., 1989. Development rates of late Quaternary soils, Silver Lake Playa, California. Soil Science Society of America Journal 53, 1127–1140.

Reid, D.A., Graham, R.C., Southard, R.J., Amrhein, C., 1993. Slick spot soil genesis in the Carrizo Plain, California. Soil Science Society of America Journal 57, 162–168.

Rhoades, J.D., 1982. Soluble salts. In: Page, A.L., Miller, R.H., Keeney, D.R. (Eds.), Methods of Soil Analysis: Part 2. Agronomy Monographs: No. 9, 2nd ed. ASA, Madison, WI, pp. 167–179.

Rostagno, C.M., 1989. Infiltration and sediment production as affected by soil surface conditions in a shrubland of Patagonia, Argentina. Journal of Range Management 42, 382–385.

Rostagno, C.M., del Valle, H.F., Videla, L., 1991. The influence of shrubs on some chemical and physical properties of an aridic soil in north-eastern Patagonia, Argentina. Journal of Arid Environments 20, 179–188.

Schoeneberger, P.J., Wysocki, D., Benham, E.C., Broderson, W.D., 2002. Fieldbook for Describing and Sampling Soils, v2.0. Natural Resources Conservation Service, National Soil Survey Center, Lincoln, NE.

Smith, B.J., McGreevy, J.P., 1983. A simulation study of salt weathering in hot deserts. Geografiska Annaler. Series A. Physical Geography 65, 127–133.

Smith, S.D., Herr, C.A., Leary, K.L., Piorkowski, J.M., 1995. Soil–plant water relations in a Mojave Desert mixed shrub community: a comparison of three geomorphic surfaces. Journal of Arid Environments 29, 339–351.

Soil Survey Division Staff, J.M., 1993. Soil Survey Manual. USDA Handbook, vol. 18. U.S. Government Printing Office, Washington, DC.

Springer, M.E., 1958. Desert pavement and vesicular layer of some soils of the desert of the Lahontan Basin, Nevada. Soil Science Society of America Proceedings 22, 63–66.

Szabolcs, I., 1979. Review of Research on Salt-Affected Soils. UNESCO, Paris, France.

Tromble, J.M., Renard, K.G., Thatcher, A.P., 1974. Infiltration for three range land soil–vegetation complexes. Journal of Range Management 27, 318–321.

Turrin, B.D., Dohrenwend, J.C., Drake, R.E., Curtis, G.H., 1985. K–Ar ages from the Cima volcanic field, eastern Mojave Desert, California. Isochron-West 44, 9–16.

Tyler, S.W., McKay, W.A., Mihevc, T., 1994. Impacts of the root zone on tracer transport. Soil Science Society of America Journal 58, 25–31.

Vasek, F.C., Barbour, M.G., 1988. Mojave desert scrub vegetation. In: Barbour, M.G., Major, J. (Eds.), Terrestrial Vegetation of California. Special Publication No. 9. California Native Plant Society, Sacramento, CA, pp. 835–867.

Weisbrod, N., Nativ, R., Adar, E.M., Ronen, D., 2000. Salt accumulation and flushing in unsaturated fractures in an arid environment. Ground Water 38, 452–461.

Wells, S.G., Dohrenwend, J.C., McFadden, L.D., Turrin, B.D., Mahrer, K., 1985. Late Cenozoic landscape evolution on lava flow surfaces of the Cima volcanic field, Mojave Desert, California. Geological Society of America Bulletin 96, 1518–1529.

Wells, S.G., McFadden, L.D., Poths, J., Olinger, C.T., 1995. Cosmogenic ^{3}He surface-exposure dating of stone pavements: implications for landscape evolution in deserts. Geology 23 (7), 613–616.

Wilcox, B.P., Wood, M.K., Tromble, J.M., 1988. Factors influencing infiltrability of semiarid mountain slopes. Journal of Range Management 41, 197–206.

Wood, Y.A., Graham, R.C., Wells, S.G., 2002. Surface mosaic map unit development for a desert pavement surface. Journal of Arid Environments 52, 305–317.

Yair, A., Lavee, H., Greitser, N., 1997. Spatial and temporal variability of water percolation and movement in a system of longitudinal dunes, western Negev, Israel. Hydrological Processes 11, 43–58.